AIAA JOURNAL
Vol. 42, No. 8, August 2004

Flowfield and Mixing Control of an Underexpanded Jet

S. Murugappan* and E. Gutmark†
University of Cincinnati, Cincinnati, Ohio 45221-0070

Flowfield and schlieren flow visualization were used to study the growth rate and mixing characteristics of a self-excited underexpanded jet. The underexpanded jet was excited at three characteristic frequencies that correspond to the initial instability, a preferred mode, and a subpreferred mode. The spreading rate and turbulent flow characteristics resulting from the three excitation frequencies were compared with the unforced baseline case. Axial and radial mean and fluctuating velocity components in the flow along with time-averaged schlieren images indicated that the growth rate and turbulence level in the jet near field could be controlled independently by exciting the jet at the different characteristic modes of the jet. The effects of forcing on mixing and spreading rates were minimal in the jet far field. The forced underexpanded jet exhibited characteristics that are strikingly similar to those obtained earlier in subsonic jets. It was observed that forcing the underexpanded jet at its preferred mode increased the spreading rate and turbulence intensity in the jet near field. Forcing the high-speed jet at frequencies close to the initial jet frequency minimizes the spreading rate of the jet. Excitation at the subpreferred mode frequency results in an increased near-field jet growth rate when compared to the preferred mode. Both the axial and radial turbulence intensity increased by 35–40% around the jet core at a subpreferred mode forcing of Sr_D = 0.09 as compared to the forcing near the initial instability frequency Sr_θ = 0.0085 and at the baseline frequency.

Nomenclature

D_j	=	diameter of the jet
f	=	frequency
P_s	=	static pressure
P_∞	=	ambient pressure, 1 atm
R	=	jet pressure ratio, P_s/P_∞
$r_{0.1}$	=	jet width based on radial distance to 10% of centerline mean velocity
$r_{0.5}$	=	jet width based on radial distance to 50% of centerline mean velocity
Sr_D	=	Strouhal number, (fD_j/U_0)
Sr_θ	=	Strouhal number, $(f\theta/U_0)$
U, V	=	axial and radial components of mean velocity
U_{CL}	=	centerline mean axial velocity
U_0	=	centerline mean axial velocity at $x/D_j = 0$
u', v'	=	axial and radial components of the turbulent velocity
u'_{CL}, u'_{SL}	=	axial component of the turbulent velocity on the centerline and shear-layer, respectively
x	=	axial distance measured from the jet exit
$\Delta r_{0.1}/\Delta x$	=	spreading rate based on $r_{0.1}$
θ	=	initial momentum thickness of the jet shear layer at the nozzle exit

Introduction

IN high-speed propulsion systems such as scramjets, factors such as combustion efficiency, reduction of emissions, improved flammability limits, and noise reduction are all governed by the completeness of the mixing process between fuel and air. One of the technical issues that is important in a scramjet combustor is the rapid mixing between fuel and air due to the limited time and space available for mixing and reaction. A major difficulty encountered when fuel is injected perpendicular to crossflow air is achieving simultaneous penetration of the fuel jet into the high-speed airstream and intense mixing between them at the molecular level to ensure efficient combustion. An added level of complexity arises due to the effect of compressibility, which reduces mixing rates at elevated convective Mach numbers ($M_c > 0.4$) (Ref. 1).

A comprehensive review of mixing enhancement techniques in supersonic flows can be found in Ref. 2. Passive mixing enhancement techniques could be broadly classified into two categories. The first is based on geometric modifications of the flowpath, and the second is based on self-excited devices that force the flow passively with no additional external energy required. A few examples of the first case involve using swirl,[3] lobed mixers[4] and splitter plates,[5] vortex generators,[6] noncircular jets,[7] and multistep jets.[8] These passive control techniques, which involve geometric modifications, could be used efficiently to improve mixing or growth rates, but the range of operating conditions for which their performance is superior to a generic circular nozzle is limited.

The second case of passive mixing enhancement techniques involves self-excitation devices. The self-excitation methods produce controlled forcing of the flow at a desired frequency and amplitude that is optimal to affect growth rates and turbulence level. These methods were extensively studied in subsonic flows, and physical insight gained from these studies can be applied to high-speed flows.[9–11] The following section deals with the strategies used in subsonic flows to control penetration and mixing as background to high-speed flow passive excitation.

In subsonic flows, the spatial evolution of jets is determined by flow instability properties and the resulting vortex dynamics.[9] The circumferential shear layer of a jet exiting from a nozzle rolls up into small-scale vortices whose length scale is determined by the initial instability frequency, which depends on exit velocity U_0 and initial shear layer thickness θ. The initial instability frequency is characterized by a Strouhal number $Sr_\theta = f \times \theta/U_0$ in the range of 0.009–0.018 (Refs. 9 and 10). These vortices interact and merge in a process that governs the spreading rate of the jet. Excitation at the initial instability frequency prevents vortex merging and, thus, minimizes the jet-spreading rate. After several mergings, the vortices evolve into large-scale structures that are called the jet preferred mode vortices. The preferred mode of the jet is defined by a Strouhal number $Sr_D = fD_j/U_0$, which is typically in the range of 0.2–0.5 in subsonic jets.[12] Forcing the jet at the preferred mode enhances vortex merging, hence accelerating the spreading rate and mixing. Exciting a jet at a frequency that is lower than the preferred mode

Presented as Paper 2003-0370 at the 41st Aerospace Sciences Meeting, Reno, NV, 7 January 2003; received 24 July 2003; revision received 29 March 2004; accepted for publication 31 March 2004.

*Research Assistant, Department of Aerospace Engineering, 745, Baldwin Hall. Member AIAA.
†Professor, Ohio Eminent Scholar, Department of Aerospace Engineering, 745, Baldwin Hall. Associate Fellow AIAA.

causes the vortices to coalesce together in a process called collective interaction, thus, further enhancing the spreading rate in subsonic jets.[9]

Similar to growth rate control of subsonic jets using flow instabilities, the goal of this paper is to apply these methods to supersonic flows. Previous studies on compressible jets indicate that the most amplified frequency would correspond to $Sr = 0.2$–0.3 (Refs. 1, 13, and 14). Because the Strouhal number remains nearly the same as in subsonic jets, the instability frequency is much higher in supersonic jet. Michalke[13] and others showed that the growth rate of flow instabilities and, therefore, the growth rate of supersonic shear layers decrease with increasing Mach number ($M > 0.4$). Therefore, excitation of supersonic jets requires actuators that can be effective at both high frequency and amplitude. This excludes the use of mechanical actuators that are limited in their frequency response or electrical actuators that require an external energy source. The following section describes acoustic-based methods that were chosen to achieve the desired passive excitation discussed in the present work.

Cavities have been widely used as self-excitation devices because flow interactions with the cavity can produce acoustic resonance. Depending on the orientation of the cavity relative to the flow, they can be classified as flow-grazing cavities or inflow cavities. Yu and Schadow[15] used grazing-flow cavities to induce formation of large-scale vortices in supersonic jets, thereby enhancing the spreading rate and reducing the afterburning flame's length and intensity. Hartmann and Trolle[16] developed a device that was later called the Hartmann–Sprenger (H–S) tube, which consists of an underexpanded jet and an inflow cavity. The device is compact and produces large-amplitude rapid pulsations when the cavity is placed within the regions in the underexpanded jet where pressure is increased behind the reflecting shock waves.[16,17] Raman et al.[18] developed a powered resonance tube bank (PRTB) actuator, which integrates a number of H–S tubes into a single device. Kastner and Samimy[19] and Samimy et al.[20] developed a Hartmann tube fluidic actuator (HTFA) that was similar to an H–S tube except that most of the area between the jet and cavity was shielded to produce a pulsating jet that was used for flow control. They observed that the distance between the jet and the cavity was a critical parameter in directing the pulsating jet out of the HTFA. Phase-averaged flow images showed that the pulsating flow was rich in vortical structures.

The current study involves application of a self-resonant passive control method to modify the spreading rate of an underexpanded jet by exciting it at different frequencies corresponding to various unstable modes. A high-frequency actuator (HFA) was used to achieve this control authority. The HFA, which is based on the concept of the H–S tube, is capable of producing high-amplitude [sound pressure level (SPL) $\approx$ 135 dB] and high-frequency (2–35-kHz) pressure and velocity oscillations. Two-dimensional velocity data and time-averaged schlieren flow visualization have been used to study the spreading rate and mixing characteristics of the underexpanded jet for excitation at the initial instability and preferred and subpreferred modes of the jet.

Experimental Setup

The HFA used to force the supersonic jet in the present experiments is a passive self-excited device. The input to the actuator is a constant air mass flow rate at a certain pressure and temperature. The output is a circular jet with fluctuating flow superimposed on the mean field. The underexpanded air jet with the integrated HFA is shown in Fig. 1. An H–S tube is the internal excitation device upstream of the supersonic jet nozzle with an exit diameter D_j of 15.25 mm. The internal H–S excitation device was held together by struts inside the nozzle. The presence of struts caused an initial perturbation in the flow, which decayed past 0.8 jet diameters. Different parameters of the H–S tube include jet diameter D_u, cavity diameter D_c, cavity length L_c, and standoff distance between the jet and the cavity X. A parametric study of these parameters was conducted in Ref. 21 to optimize D_u, D_c, and X. In the current study, D_u, D_c, and X were kept fixed, cavity length L_c was alone varied

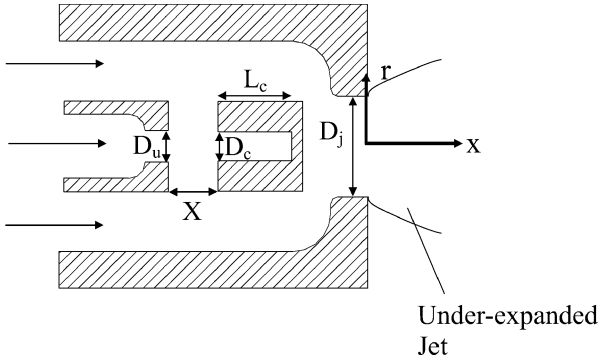

Fig. 1 Schematic of HFA.

to excite different frequencies. The jet was operated at two different pressure ratios corresponding to fully expanded Mach numbers M of 1.57 and 2.07. Three different forcing frequencies were used to evaluate the growth rate of the jet. An unforced baseline jet was used to compare with the excitation at three frequencies: initial instability $Sr_\theta = 0.0085$, a preferred mode $Sr_D = 0.27$, and a subpreferred mode $Sr_D = 0.09$.

A two-dimensional laser Doppler velocimeter (LDV) system was used to measure the axial and radial velocity components. A Laskin nozzle using olive oil was used to seed the flow. The geometrical mean diameter of the seeding particles was approximately 0.5 μm. The Stokes number ST_x is given by

$$ST_x = \tau_p/\tau_f$$

where τ_p and τ_f are the particles and flow timescales, respectively,

$$\tau_p = \left(\rho_p D_p^2 \big/ 18\mu\right)^* (1 + 2.7^* \text{Knudson number})$$

$$\text{Knudson number} = L_m/D_p,$$

$$\tau_f = \delta/U_{\text{CL}}$$

where ρ_p is the particle density, D_p is the particle diameter, μ is the absolute viscosity of the air, L_m is the length of mean free path of the molecule, δ is the shear layer thickness, and U_{CL} is the velocity on the centerline.

The upper bound of Stokes number in the present experiments was 0.059. Computations of Samimy and Lele[22] for a particle-laden compressible mixing layer suggest that the Stokes number defined using vorticity thickness should be less than 0.5 for correct flow visualization. When the incompressible result that the visual thickness is about twice the vorticity thickness is used, the Stokes number using the shear layer thickness should be below 0.25 (Ref. 23). The current data are obtained for Stokes number that are well below 0.25.

The LDV system used a 300-mW argon-ion laser. The signal processor had a 180-MHz Doppler frequency upper limit for high-speed flow measurements and a 120-MHz bandwidth for high-turbulence measurements. The transmitter is a 60-mm probe with beam-splitting and frequency-shifting optics. The diameter of the measuring volume was set to 1.00 mm. The minimum spacing between two measurement locations was set to 1.27 mm, which was greater than the probe volume diameter to avoid any spatial overlap between data points. Velocity bias is an error inherent in the statistical analysis of burst measurements from LDV. Different types of correction techniques such as inverse velocity magnitude,[24] particle interarrival time,[25] and particle residence time[26] have been used in the past to account for the statistical bias of the particle arrival and measurement probability in the probe volume of the LDV. The current experiments did not employ any velocity debiasing in the data reduction process. Comparison of mean axial and radial velocity profiles obtained in the current study without velocity bias (particle residence time weighting) indicates a maximum of less than 1% error.

The jet was attached to a biaxial-slide three-dimensional traverse. A LABVIEW program was used to synchronize the traverse with the signal processor. A transistor-transistor-logic (TTL) signal sent from the signal processor after recording the velocity at a certain location initiated the movement of the traverse to the next position. After a predetermined time, the laser Doppler anemometer (LDA) recorded the data. This process continued until the entire flowfield spanning 16 jet diameters downstream was measured. The bislide traverse had a straight line accuracy of 0.015% and a repeatability of 0.001% of the full range of the traverse. Experimental errors for the LDA were largely governed by finite sampling times. Data rates of the LDV were as high as 40 kHz with a 90% validation rate near the axis and lower elsewhere.

Time-averaged schlieren images were used as diagnostic tools to evaluate the spreading rate of the excited underexpanded jet. The schlieren setup consisted of two 15.24-cm parabolic mirrors with a focal length of 1.524 m. An arc lamp was used as a continuous light source. The light beam was collimated through the mirror, and the image was cut at the focal point by a knife-edge before being captured by a charge-coupled device (CCD) camera. The camera had a 512×512 pixel thinned, scientific grade CCD. The exposure time was set to 0.01 s. A microphone placed at 10 in. upstream at an angle of 45 deg to the HFA was used to record the acoustic pressure produced by the actuator.

In the current experiments, velocity data in the flow were acquired at $M = 1.57$. The schlieren images were taken at higher $M = 2.07$ so that the density gradient could be enhanced in the images.

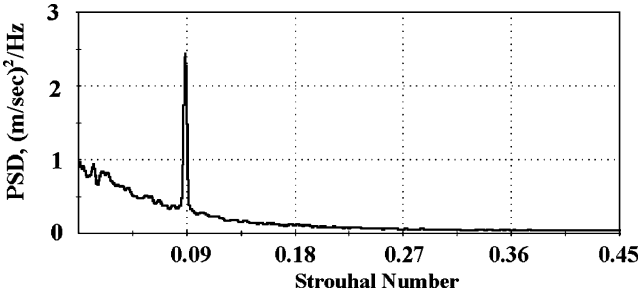

Fig. 2a Axial velocity PSD at $M = 1.57$, $Sr_D = 0.09$, and $x/D_j = 2.5$.

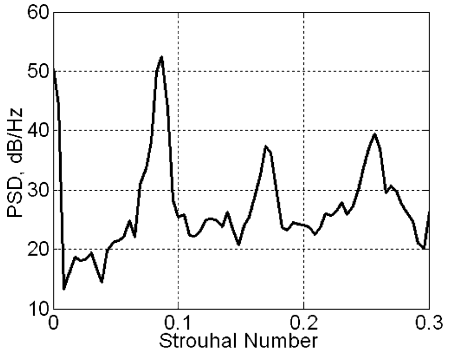

Fig. 2b Acoustic pressure PSD at $M = 1.57$, $Sr_D = 0.09$, and $x/D_j = 16.7$, 45 deg upstream.

Results and Discussion

Velocity and acoustic pressure power spectral density (PSD) of the $M = 1.57$ supersonic jet forced at a frequency of $Sr_D = 0.09$ are shown in Fig. 2. The velocity spectra were measured on the centerline at $x/D_j = 2.5$. Both velocity and pressure spectra show a dominant peak at the excitation frequency. It was observed that the SPL initially increases from 118 to 125 dB with increasing M for the baseline, $Sr_\theta = 0.0085$, and $Sr_D = 0.09$ cases (Fig. 3). For values of M greater than 1.3 and less than 2, the change in SPL was minimal for the baseline and $Sr = 0.09$ case. The trends in SPL and the amplitude level for the three cases were similar. Hence, the excitation frequency alone played an important role in modifying the flow characteristics of the HFA jet. The mechanism used to control the spreading rate and mixing characteristics is based on exciting certain instabilities in the shear layer. The Mach numbers at which the LDV and schlieren measurements were performed are indicated in Fig. 3.

Mean Velocity Flow (U and V)

Figures 4a–4c and 5a–5c are plots of mean axial and radial velocities for the baseline and two forcing cases ($Sr_D = 0.09$ and $Sr_\theta = 0.0085$) at different axial locations. Figures 4a–4c and 5a–5c show U/U_{CL}, where the mean velocity U was normalized by the maximum mean axial velocity on the centerline, U_{CL}, at every axial location as a function of normalized radial distance. The radial distance r was normalized by the jet half-width, $r_{0.5}$. The HFA jet was axisymmetric; hence plots in Figs. 4a–4c and 5a–5c are shown along one radius. Note that the axial mean velocity plots in Figs. 4a–4c and 5a–5c collapse into to single curve past 5 jet diameters for all the cases. The present data are compared here to a subsonic circular jet measured at a distance of 40–97 diameters from the nozzle.[27] Additional comparison is made with an overexpanded jet at $M = 1.54$ (Ref. 28) and with an ideally expanded $M = 2$ jet (Ref. 29). Note that in spite of the very different flow conditions of the far field, the subsonic jet[27] and the near-field overexpanded jet[28] show good agreement with the current near-field measurements of the underexpanded jet; the fully expanded jet[29] deviates somewhat from both.

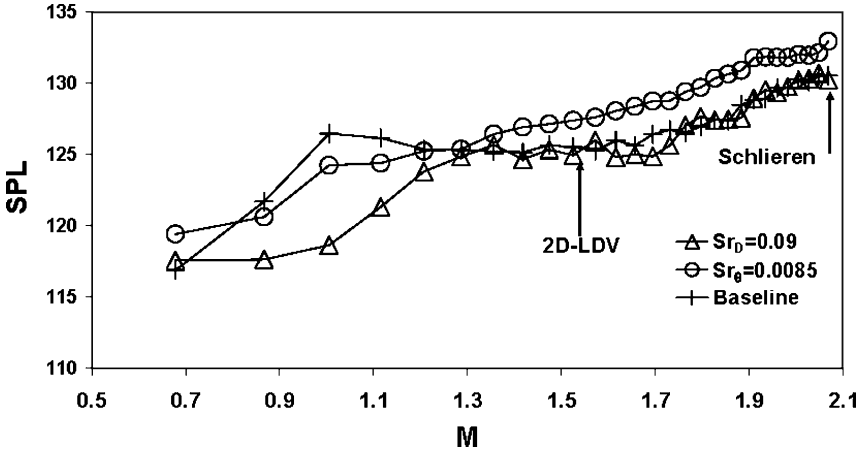

Fig. 3 SPL of the HFA for baseline, $Sr_\theta = 0.0085$ and $Sr_D = 0.09$ as a function of Mach number.

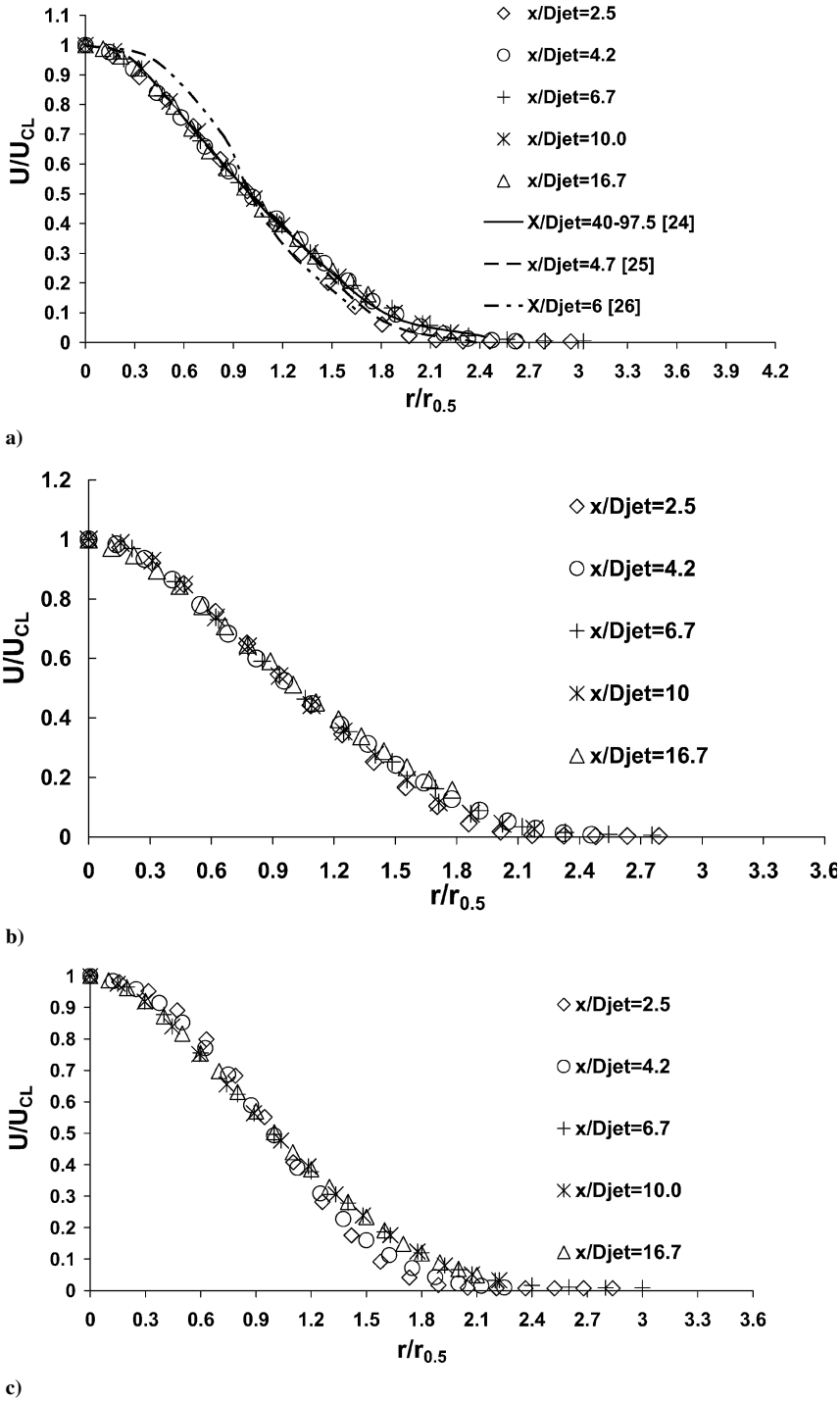

Fig. 4 Mean axial velocity for a) baseline, b) Sr_θ = 0.0085, and c) Sr_D = 0.09.

The radial mean velocity for all of the cases was found to be no more than 10% of the maximum mean axial velocity. The subsonic jet data show significantly lower radial velocity compared to the typical behavior of an underexpanded jet that tends to expand as it exits the nozzle. The maximum mean radial velocity for the subpreferred mode case was found to be approximately twice that of the baseline (Fig. 5c compared to Fig. 5a). This indicates higher spreading rate with the subpreferred mode forcing.

Fluctuating Velocity Flow (u' and v')

Figures 6a–6c and 7a–7c are plots of axial and radial turbulent velocities for the baseline and two forcing cases ($Sr_D = 0.09$ and $Sr_\theta = 0.0085$) at different axial locations. The turbulent velocities have been normalized by the maximum mean axial velocity on the centerline at every axial location. The turbulent intensity of the axial component of all three cases increases in the downstream direction, approaching a self-similar profile. The normalized axial turbulence intensity agrees very well with the far-field data of the subsonic jet.[27] The agreement with the radial turbulent velocity is also quite good.[27] The differences relative to the $M = 1.54$ overexpanded jet[28] and ideally expanded $M = 2$ (Ref. 29) jet can be attributed to the expected differences between the present underexpanded jet and the overexpanded and fully expanded jets in the other two references.

There was nearly a 35% increase in axial turbulence intensity for the $Sr_D = 0.09$ case as compared to the other two (Fig. 6). The

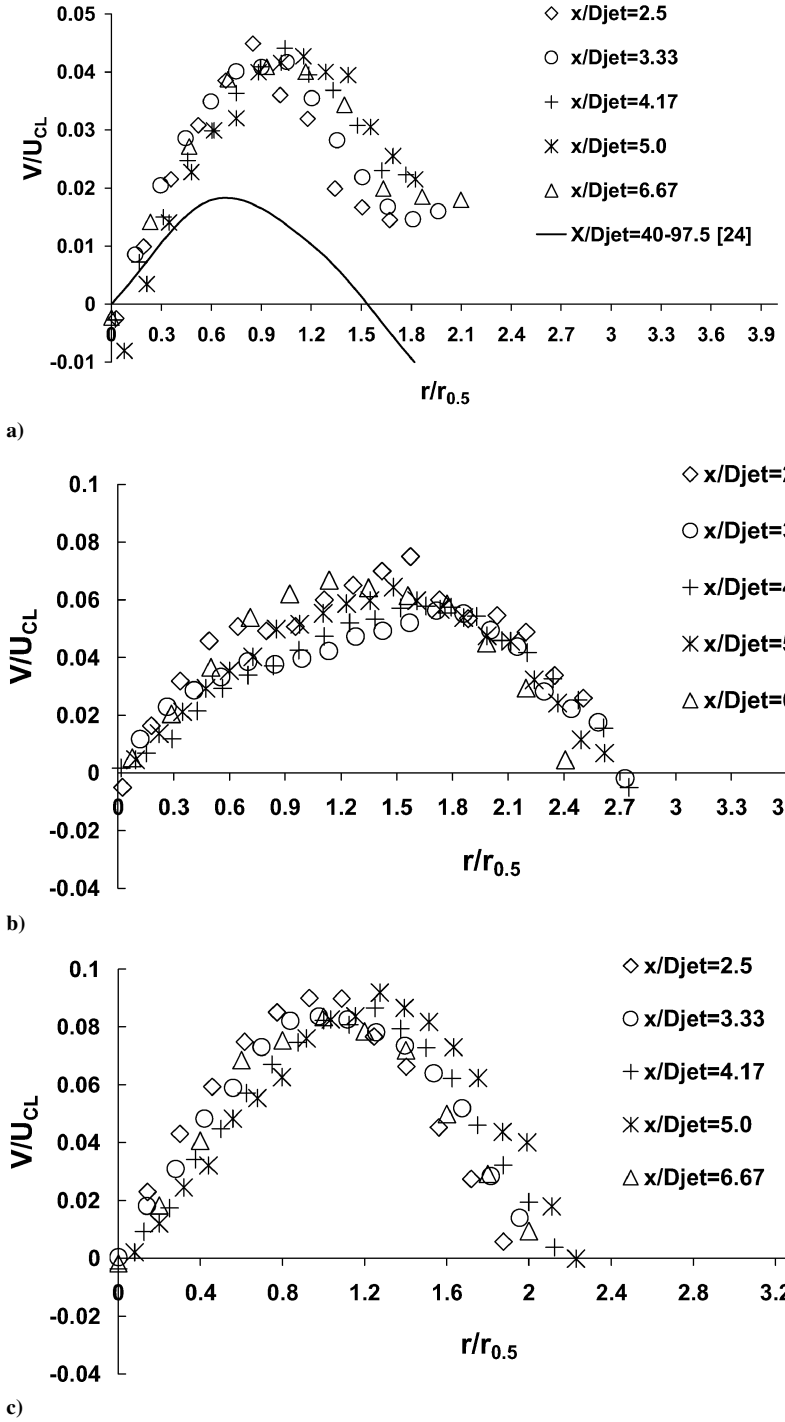

Fig. 5 Mean radial velocity for a) baseline, b) Sr_θ = 0.0085, and c) Sr_D = 0.09.

axial turbulent velocity plots (Figs. 6) approach a self-preserving form past 10 jet diameters, whereas the turbulent radial component (Figs. 7) does not attain the self-similar form even at 17 jet diameters, which is the farthest axial measurement point. In a subsonic jet the turbulent axial component reaches self-similarity at $x/D_j > 40$, whereas the radial component reaches self-similarity only at $x/D_j > 70$ (Ref. 27). Wygnanski and Fiedler[27] proposed that the approach to equilibrium in a jet takes place in steps. The mean velocity becomes similar at $x/D_j > 20$, which leads to a certain production of u', and after a balance is reached in the major flow direction, equilibrium is attained in other directions. A similar trend was observed in the present measurements.

The axial turbulence intensity was observed to be higher than its radial counterpart for all of the cases. The fluctuation levels reached a maximum of 32 and 21% on the jet centerline for the axial and radial directions. Both axial and radial turbulence intensities for $Sr_D = 0.09$ were higher in the central region of the jet than that of the baseline or $Sr_\theta = 0.0085$. This indicates more intense mixing with forcing at $Sr_D = 0.09$ near the jet core.

Spreading Rate and Mixing Characteristics

Normalized centerline mean axial velocity decay plots are shown in Fig. 8 in terms of U_0/U_{CL}. The mean velocity decay rates of the baseline jet and the jet forced at $Sr_\theta = 0.0085$ are very similar with a slightly reduced rate of the forced jet. Forcing the underexpanded jet at the subpreferred mode resulted in increased decay rate only in the near field of the jet ($x/D_j < 6$) but no changes

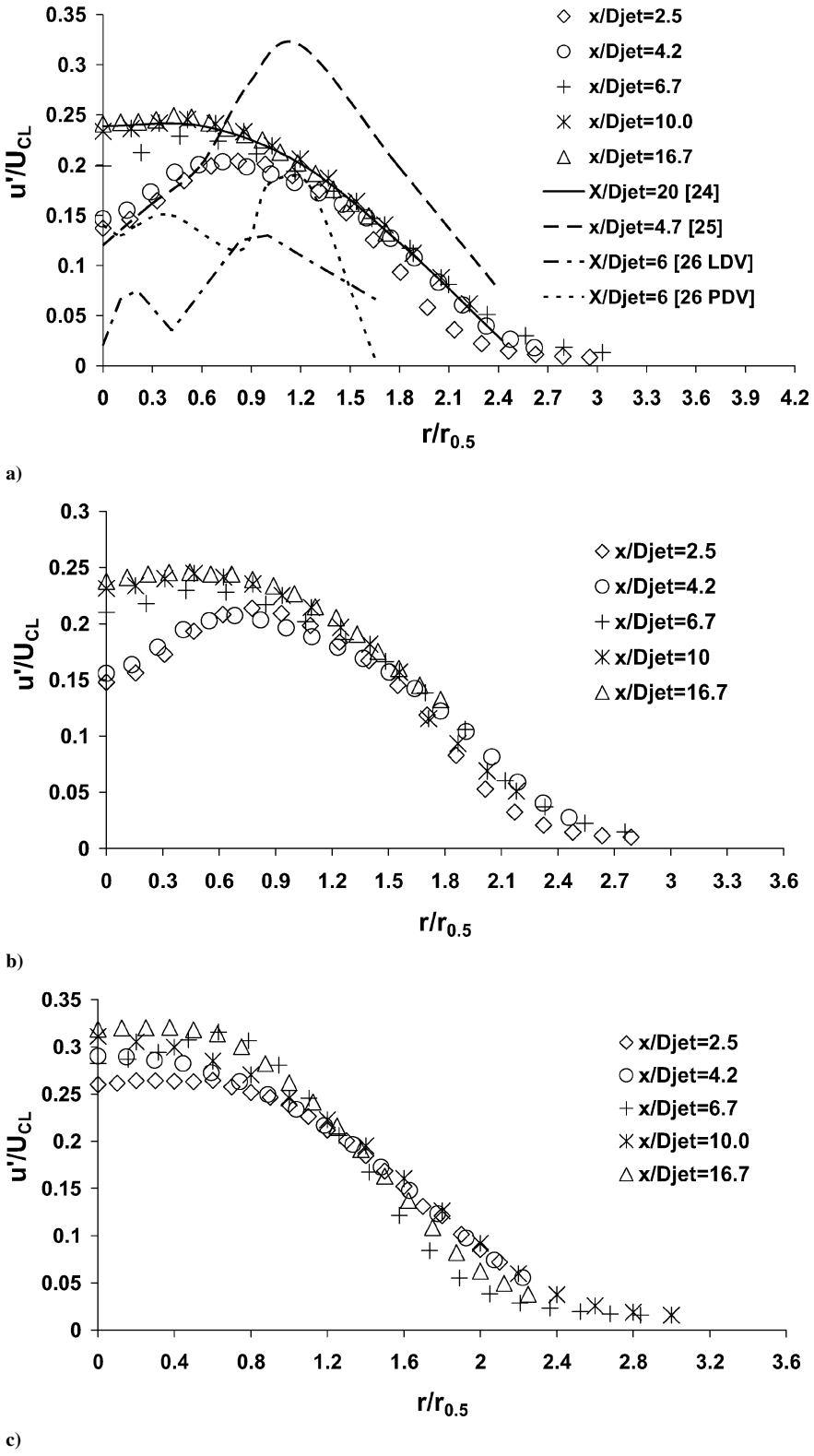

Fig. 6 Axial rms velocity for a) baseline, b) $Sr_\theta = 0.0085$, and c) $Sr_D = 0.09$.

in the decay rate in the far field ($x/D_j < 6$). The forcing, thus, produced only a shift in the virtual origin of the jet with no other changes found in the centerline mean velocity decay in the far field of the jet.

Time-averaged schlieren images are presented for all of the cases, in Fig. 9. Because the schlieren visualization is based on density gradients, the boundaries are not visible as soon as mixing with the ambient flow occurs. For this reason, the baseline and the jet forced at $Sr_\theta = 0.0085$ (Figs. 9a and 9b) show apparent reduction in width. Comparison between these two jets shows a slight reduction in the jet-spreading rate due to forcing. Figures 9c and 9d, which correspond to the $Sr_D = 0.27$ and 0.09 forcing, show that the size of the shock cells is reduced, indicating that the jet velocity is decreased and that a more uniform density gradient was obtained relative to the baseline and $Sr_\theta = 0.0085$ cases. The spreading rate of the jets forced at the preferred mode and subpreferred

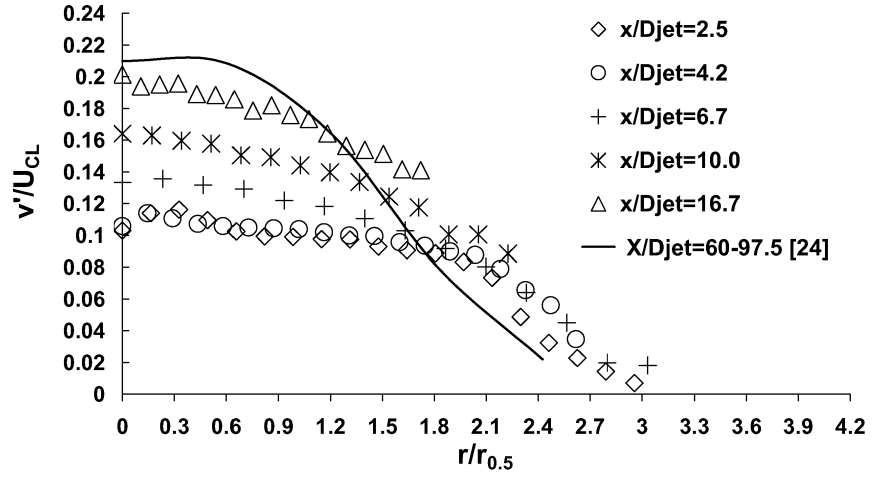

a)

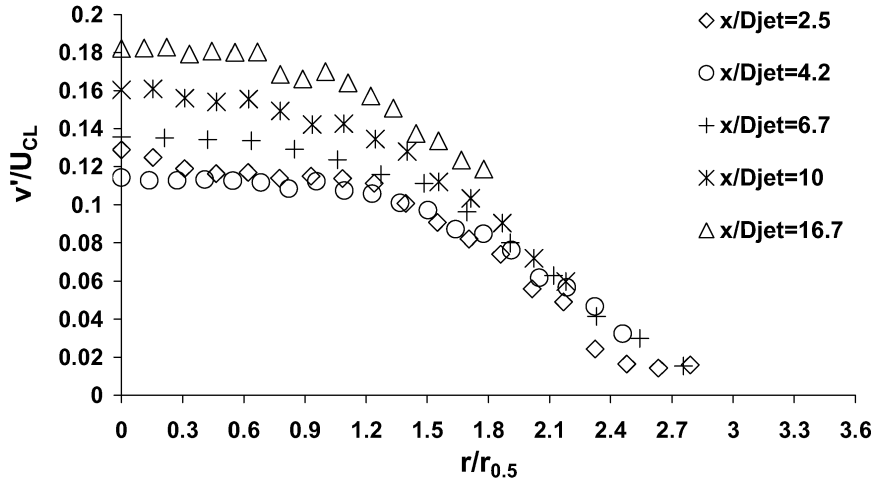

b)

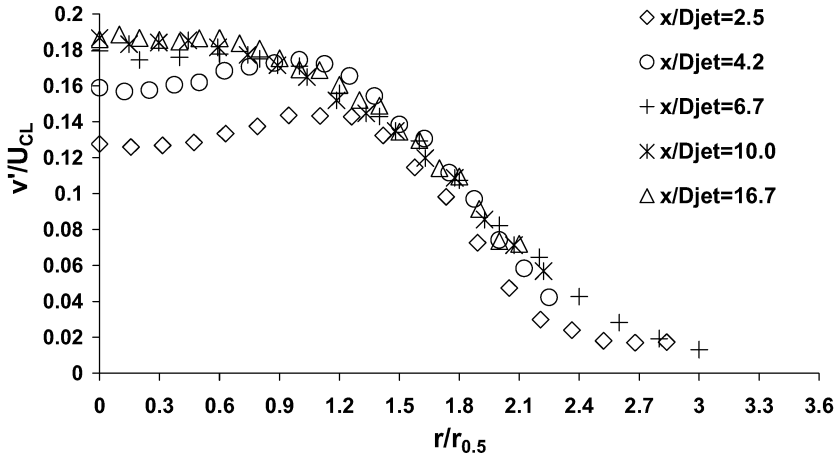

c)

Fig. 7 Radial rms velocity for a) baseline, b) Sr_θ = 0.0085, and c) Sr_D = 0.09.

mode increased relative to the other two, as indicated by the dashed lines.

Figures 10a and 10b are the normalized axial turbulent velocities along the centerline and the shear layer, for the baseline and three forced cases. The effect of forcing caused variations in centerline and shear layer turbulent intensity levels only in the jet near field ($x/D_j < 6$) with no discernible effect in the jet far field ($x/D_j > 6$). The $Sr_D = 0.09$ case has low mean centerline axial fluctuating velocity until $x/D_j = 1.25$, when compared to all other cases. The centerline axial fluctuating velocity doubled at 2.5 jet diameters for $Sr_D = 0.09$ as compared to the baseline case. The $Sr_D = 0.09$ case also shows a 55% maximum increase in turbulent fluctuations in the shear layer as compared to the baseline and $Sr_\theta = 0.0085$ case. This indicates enhanced mixing of the jet with the ambient fluid in the near field of the jet. This supports the observation of enhanced mixing in the jet core from the centerline axial mean velocity decay plots (Fig. 8). The preferred mode of the jet, $Sr_D = 0.27$, shows higher turbulence intensity than both the baseline and $Sr_\theta = 0.0085$

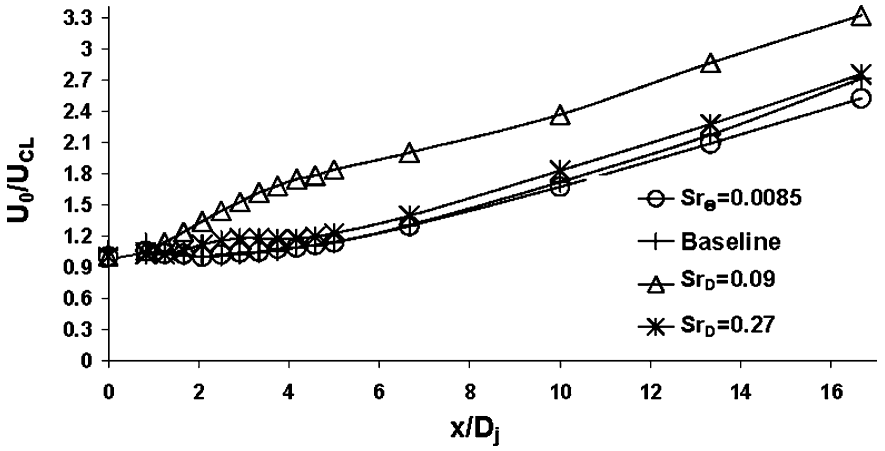

Fig. 8 Normalized centerline mean axial velocity decay, U_0/U_{CL}, and variation with x/D_j.

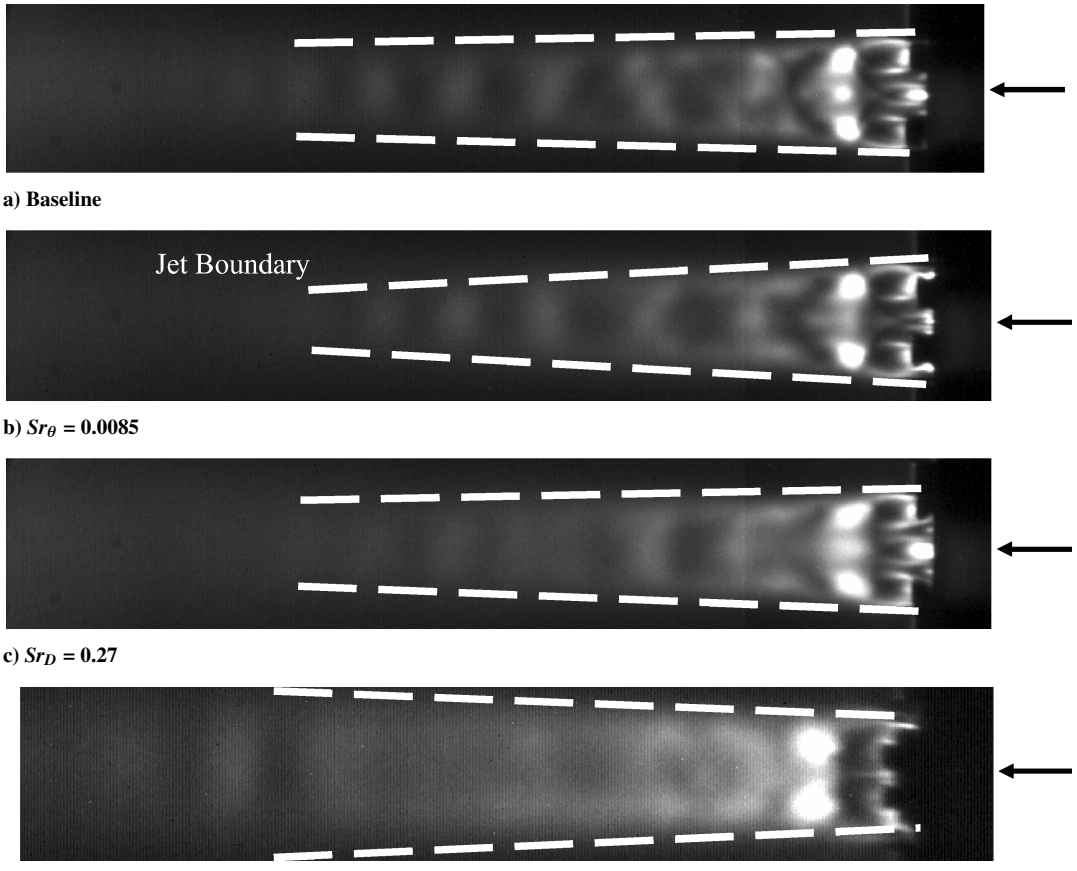

a) Baseline

b) Sr_θ = 0.0085

c) Sr_D = 0.27

d) Sr_D = 0.09

Fig. 9 Time-averaged schlieren images at M = 2.1.

case but was lower than $Sr_D = 0.09$. This indicates that forcing at a frequency lower than the preferred mode causes large increases in turbulence fluctuations and spreading rate in the near field.

Comparison of the normalized 10% jet width $r_{0.1}$ for the four different cases is shown as a function of the axial locations in Fig. 11. The jet width $r_{0.1}$ is defined as the radial distance from the jet centerline to the point at which the jet mean velocity drops to 10% of the mean velocity level on the centerline at this axial location. Here $r_{0.1}$ was selected to represent the jet width because the schlieren images (Fig. 9) showed that much of the spread is at the outer radial regions of the jet. A comparison at $r_{0.5}$ showed smaller differences between the four cases in the far field compared to $r_{0.1}$. It was observed that in the first six jet diameters there was a 78% increase in the slope with the subpreferred mode as compared to the initial instability case. In the far field $6 < x/D_j < 17$, the differences between the spreading rates are much lower, and the low-frequency forcing case corresponding to $Sr_D = 0.09$ shows up to 25% increase in slope as compared to forcing at the preferred mode. This supports the suggestion that forcing the high-speed jet at a frequency lower than the preferred mode causes vortices to form at the excitation frequency. In subsonic flows, the vortices coalesce together in a process called collective interaction[10] such that the passage frequency is governed by the forcing function. In supersonic flows, excitation at the preferred mode could amplify the vortex interaction process, resulting in enhanced mixing and growth rate. The forced case that corresponds

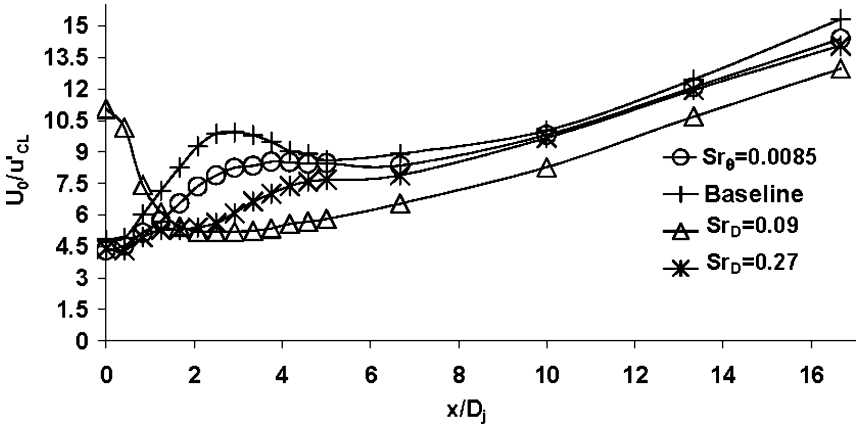

Fig. 10a Normalized axial turbulence intensity along the centerline.

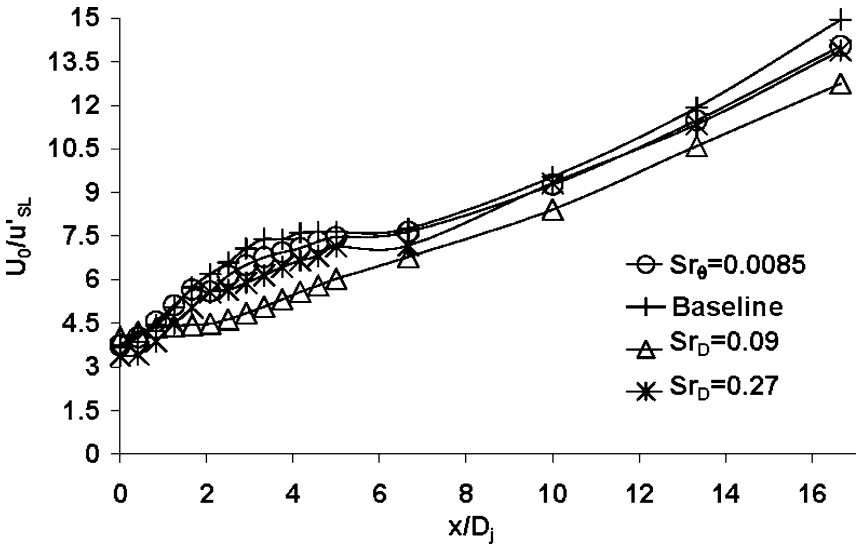

Fig. 10b Normalized axial turbulence intensity in the shear layer.

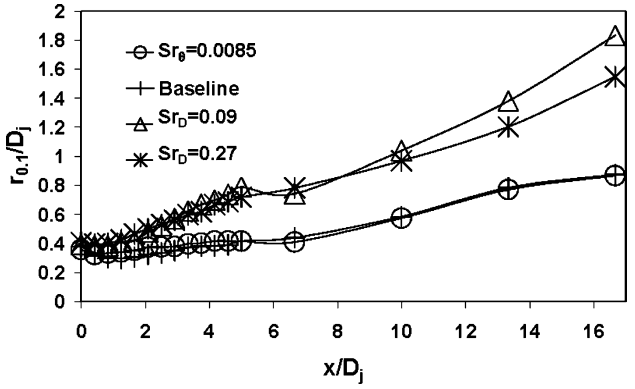

Fig. 11 Normalized jet width based on radial distance to reach 10% of the mean centerline velocity, at different axial locations.

to the initial instability could suppress vortex interaction, hence, resulting in reduced jet spread and mixing.

Conclusions

The impact on mixing and growth rate of an underexpanded jet forced at the initial instability, preferred mode, and subpreferred mode was studied. The mean axial and radial velocities exhibited a self-preserving form downstream of five jet diameters for all of the cases. Both the mean and turbulent velocity profiles agreed well with those of the subsonic circular jet.[27] The effect of the forcing caused changes in the spreading rate, turbulent intensity levels, and mean axial velocity decay only in the near field of the jet ($x/D_j < 6$). The changes in the far field ($x/D_j > 6$) between the forced and baseline cases were minimal. Forcing the jet at the initial instability reduced spreading rate and turbulent mixing in the shear layer and around the core. This was possibly a result of suppressed vortex interaction, as also observed in subsonic flows.

Exciting the underexpanded jet at the preferred mode or at a frequency below the preferred mode resulted in fast dissipation of the shock cells. The spreading rate and mixing characteristics were enhanced. Forcing at the preferred mode resulted in a significant increase in the jet spreading rate and turbulence intensity, in the jet near field ($x/D_j < 6$). There was a maximum of 100 and 55% increase in the centerline and shear layer axial turbulence intensity, respectively, for $Sr_D = 0.09$ excitation compared to the baseline. The overall impact of forcing on the underexpanded jet spread, mean centerline velocity decay, and turbulence was higher for the subpreferred mode frequency ($Sr_D = 0.09$) when compared to exciting the jet at its preferred mode ($Sr_D = 0.27$) in the near field.

Excitation at the initial instability frequency range ($Sr_\theta = 0.0085$) resulted in decreased mixing rate and growth characteristics of the underexpanded jet in the near field. Velocity measurements indicate a lower spreading rate, and schlieren images show a distinct diamond shock pattern near the jet core.

The response of the underexpanded jet to excitation at the initial instability, preferred mode, and subpreferred mode frequencies was remarkably similar to that of the subsonic jet. The self-excitation

method described here provides a means to manipulate the supersonic jet as required for a specific application; increased penetration into a coaxial or cross stream can be achieved by initial instability forcing, whereas increased mixing, both at large and small scales is possible by preferred mode forcing. The subpreferred mode provides the largest spread and mixing in comparison to all of the cases studied in the near field of the jet.

Acknowledgments

The financial support of the Joint Air Force Research Laboratory (AFRL)/Dayton Area Graduate Studies Institute is gratefully appreciated. The authors acknowledge J. Donbar, M. Gruber, and T.A. Jackson from AFRL/PR (Propulsion Directorate) for their help and support. We appreciate the guidance given by Russell Dimicco, for his help in data analysis and setting up the experiments. The authors thank D. Hurd of the mechanical engineering machine shop at the University of Cincinnati for fabricating the high-frequency actuator.

References

[1]Papamoschou, D., and Roshko, A., "The Compressible Turbulent Shear Layer: An Experimental Study," *Journal of Fluid Mechanics*, Vol. 197, 1988, pp. 453–477.

[2]Gutmark, E. J., Schadow, K. C., and Yu, K. H., "Mixing Enhancement in Supersonic Free Shear Flows," *Annual Review of Fluid Mechanics*, Vol. 27, 1995, pp. 375–417.

[3]Cutler, A. D., and Doerner, S. E., "Effects of Swirl and Skew upon Supersonic Wall Jet in Cross flow," *Journal of Propulsion and Power*, Vol. 17, No. 6, 2001, pp. 1327–1332.

[4]Presz, W. M., Morin, B. L., and Gousy, R., "Forced Mixer Lobes in Ejector Designs," *Journal of Propulsion and Power*, Vol. 4, No. 4, 1988, pp. 350–355.

[5]Clemens, N. T., and Mungal, M. G., "Effects of Side Wall Disturbances on the Supersonic Mixing Layer," *Journal of Propulsion and Power*, Vol. 8, No. 1, 1992, pp. 249–251.

[6]Dolling, D. S., Fournier, E., and Shau, Y. R., "Effects of Vortex Generators on the Growth of Compressible Shear Layer," *Journal of Propulsion and Power*, Vol. 8, No. 5, 1992, pp. 1049–1056.

[7]Gutmark, E. J., Schadow, K. C., and Wilson, K. J., "Noncircular Jet Dynamics in Supersonic Combustion," *Journal of Propulsion and Power*, Vol. 5, 1989, pp. 529–533.

[8]Schadow, K. C., Gutmark, E., Parr, D. M., Parr, T. P., Wilson, K. J., and Ferrell, G. B., "Enhancement of Fine Scale Turbulence for Improving Fuel Rich Plume Combustion," *Journal of Propulsion and Power*, Vol. 6, No. 4, 1990, pp. 357–363.

[9]Ho, C. M., and Huerre, P., "Perturbed Free Shear Layers," *Annual Review of Fluid Mechanics*, Vol. 16, 1984, pp. 365–424.

[10]Ho, C. M., and Huang, L. S., "Subharmonics and Vortex Merging in Mixing Layers," *Journal of Fluid Mechanics*, Vol. 119, 1982, pp. 443–473.

[11]Oster, D., and Wygnanski, I., "The Forced Mixing Layer Between Parallel Streams," *Journal of Fluid Mechanics*, Vol. 123, 1982, pp. 91–130.

[12]Gutmark, E., and Ho, C. M., "On the Preferred Modes and Spreading Rates of Jets," *Physics of Fluids*, Vol. 26, 1983, pp. 2932–2938.

[13]Michalke, A., "Survey on Jet Instability Theory," *Progress in Aerospace Sciences*, Vol. 21, 1984, pp. 159–199.

[14]Gutmark, E., Yu, K. H., and Schadow, K. C., "The Effect of Nozzle-Lip on the Structure Stability, and Pressure Fluctuations of Coaxial Supersonic Jets," AIAA Paper 93-4363, Oct. 1993.

[15]Yu, K. H., and Schadow, K. C., "Cavity Actuated Supersonic Mixing and Combustion Control," *Combustion and Flame*, Vol. 99, 1994, pp. 295–301.

[16]Hartmann, J., and Trolle, B., "A New Acoustic Generator. The Air Jet Generator," *Journal of Scientific Instruments*, Vol. 4, 1927, pp. 101–111.

[17]Hartmann, J., "Construction, Performance, and Design of the Acoustic Air-Jet Generator," *Journal of Scientific Instruments*, Vol. 16, 1939, pp. 140–149.

[18]Raman, G., Mills, A., and Othman, S., "Development of Powered Resonance Tube Actuators for Active Flow Control," *Proceedings of ASME-FEDSM, 2001 Fluids Engineering Division*, ASME FEDSM 2001-18273, American Society of Mechanical Engineers, Fairfield, NJ, 2001.

[19]Kastner, J., and Samimy, M., "Development and Characterization of Hartmann Tube Fluidic Actuators for High-Speed Flow Control," *AIAA Journal*, Vol. 40, No. 10, 2002, pp. 1926–1934.

[20]Samimy, M., Kastner, J., and Debiasi, M., "Control of a High-Speed Impinging Jet Using a Hartmann-Tube Based Fluidic Actuator," AIAA Paper 2002-2822, June 2002.

[21]Murugappan, S., and Gutmark, E., "Parametric Study of Hartmann–Sprenger Tube," AIAA Paper 2002-1012, Jan. 2002.

[22]Samimy M., and Lele, S. K., "Motion of Particles with Inertia in a Compressible Free Shear Layer," *Physics of Fluids A*, Vol. 3, 1991, pp. 1915–1923.

[23]Clemens, N. T., and Mungal, M. G., "A Planar Mie Scattering Technique for Visualizing Supersonic Mixing Flows," *Experiments in Fluids*, Vol. 11, 1991, pp. 175–185.

[24]McLaughlin, D. K., and Tiederman, W. G., "Biasing Correction for Individual Realization of Laser Anemometer Measurements in Turbulent Flows," *Physics of Fluids*, Vol. 16, 1973, pp. 2082–2088.

[25]Hoesel, W., and Rodi, W., "New Biasing Elimination Method for Laser Doppler Velocimetry Counter Processing," *Review of Scientific Instruments*, Vol. 48, 1977, pp. 910–919.

[26]Buchhave, P., and George, W. K., Jr., "Bias Corrections in Turbulence Measurements by the Laser Doppler Anemometer," *Proceedings of the Third Workshop on Laser Doppler Anemometry*, Purdue Univ., West Lafayette, IN, 1978, pp. 110–119.

[27]Wygnanski, I., and Fiedler, H., "Some Measurements in the Self Preserving Jet," *Journal of Fluid Mechanics*, Vol. 38, 1969, pp. 577–612.

[28]Smith, W., Northam, G. B., and Drummond, P., "Application of Absorption Filter Planar Doppler Velocimetry to Sonic and Supersonic Jets," *AIAA Journal*, Vol. 34, No. 3, 1996, pp. 434–441.

[29]Clancy, P. S., Samimy, M., and Erskine, W. R., "Planar Doppler Velocimetry: Three Component Velocimetry in Supersonic Jets," *AIAA Journal*, Vol. 37, No. 6, 1999, pp. 700–707.

W. Dahm
Associate Editor